

Synthesis of Ceria nanoparticles for the photocatalytic degradation of Methylene Blue dye using fruit extracts

SuvethaRani.J^{a,*}

^{a*} PG and Research Department of Physics, Thiagarajar College, Madurai, Tamilnadu-625 009, India

Nanotechnology is one of the most dynamic researches in modern materials science and technology. Eco friendly methods of green mediated synthesis of nanoparticles are the current research of nanotechnology. The present work leads to the synthesis of Ceria nanoparticles (Ceria NPs) from aqueous fruit extract of muskmelon (Cucumis melo) and watermelon (Citrulluslanatus). Synthesized nanoparticles are characterized under UV-Vis Spectroscopy and X-ray diffraction. The functional groups present in the nanoparticles are studied using FT-IR analysis. Raman spectrum of the synthesized nanoparticles confirm the fluorite cubic structure of synthesized Ceria NPs. Additionally, CeriaNPs perform well as a photo-catalyst by degrading Methylene Blue dye.

KEYWORDS: Cerium oxide nanoparticles, Muskmelon (Cucumis melo), watermelon (Citrulluslanatus), Degradation of Methylene Blue Dye, Photocatalytic activity.

Date of Submission: 10-12-2020

Date of Acceptance: 25-12-2020

I. Introduction

Green synthesis methods of nanoparticles are found to be cost effective and eco-friendly too as they reduce the effects of toxic byproducts[1]. These green synthesized nanoparticles are also shown to be stable as chemically synthesized one and the rate of synthesis is also much faster[2]. Recently researchers shown much interest on the transition metal oxides especially ceria nanoparticles owing to their wide applications in various fields like cosmetics[3], fuel cells, solar energy conversion, sensor etc[4–8]. Ceria is a cubic fluorite type of oxide with a band gap energy of 3.19eV[9].

Increase in organic pollutants in water has been observed across the world due to increase in population and development in industries and agriculture. Such pollutants pose irreversible hazards to human and aquatic life. Textile industries use many types of dyes for dyeing processes and the excess dyes are discharged into effluent streams. Thus, the effluent from textile industry needs efficient treatment technology. However, the common wastewater treatment solutions are ineffective in deteriorating the dyes due to its properties of non-biodegradable and persistent[10]. Though many conventional methods are available, low cost methods have been proven to be effective. Amongst them is transition metal oxide based photocatalytic degradation could be considered as the most efficient. Photo catalysis is a fast-developing science in which a reaction is accelerated by light. Though Ultraviolet irradiation combined with ozone or hydrogen peroxide leads to a complete destruction of the pollutants, the formation of intermediates arising from the photo degradation reaction could be more harmful than the pollutant itself. Such difficulty can be avoided by using the photocatalytic degradation. In photocatalysis, the degradation is initiated through the attack of hydroxyl radicals (OH^{*}) at the weakest chemical bonds of the dye molecules[11]. After that, the intermediates of the process will experience radical chain reaction with the oxygen molecules and eventually decompose to form water and carbon dioxide[12].

Scientists from the Indian Institute of Science, Bengaluru in India[4] have developed a novel reusable nanocomposite material, with cerium being the important element in it, which can degrade microbes and chemical dyes that are common effluents in rivers. Here, Methylene blue dye was chosen as a model dye for photocatalytic degradation as it is harmful to human health[13].

Although ceria nanoparticles were synthesized from watermelon extract in earlier[4], this work presents the green synthesis of ceria nanoparticles from muskmelon fruit extract as reducing agent for the first time. The photocatalytic degradation of MB dye using ceria NPs synthesized from muskmelon (Cucumis melo) and watermelon fruit (Citrulluslanatus) extract as catalysts has been examined.

II. Experimental details

2.1 Materials and methods

Cerium nitrate and methylene blue dye were purchased from Sigma Aldrich, India. Muskmelon and Watermelon fruits were purchased from local market, Madurai, Tamilnadu, India.

2.2 Green synthesis of Ceria nanoparticles

The Muskmelon and Watermelon fruit were crushed separately to obtain their solid juices. It is then filtered to remove solid impurities. Then the fruit extracts were stored for the synthesis of Ceria nanoparticles (CeO₂ NPs).

1:1 weight ratio of cerium nitrate and Muskmelon fruit extract was taken in a glass trough followed by the addition of 10 ml of distilled water. The solution was stirred magnetically for 10 minutes to get a homogenous solution. Then the solution was subjected to hot plate that resulted in viscous gel formation.

The next step was that the obtained gel was heated in a muffle furnace at ±300°C. Smoldering type of the reaction takes place and within 3–4 min, the nanocrystalline Ceria was obtained. Same method was followed to obtain ceria nanoparticles using watermelon fruit extract. The synthesized Ceria NPs were pale yellow in color.

2.3 Characterization

The absorbance spectra of green synthesized Ceria NPs were recorded using JASCO, UV-VIS NIR spectrometer at room temperature. The crystallinity and size of the Ceria NPs were analyzed using Powder XRD- Bruker instrument. FTIR spectra were recorded using SHIMAZDU infrared spectrophotometer (4000-400 cm⁻¹). The micro-Raman spectra were recorded at room temperature using a laser Raman confocal microprobe (LabRam HR 800).

2.4 Degradation and adsorption kinetics experiment of MB on Ceria NPs

Typically, 0.001g of Methylene blue dye was added to 100mL of double distilled water used as stock solution. 0.001g of synthesized Ceria nanoparticles was added to 100mL of Methylene blue dye solution. A control was also maintained without addition of Ceria nanoparticles. Before exposing to irradiation, the reaction suspension was well mixed by being magnetically stirred for 1 hour to clearly make the equilibrium of the working solution. Afterwards, the dispersion was put under the sunlight and monitored. Aliquots of solution (~5 mL) were withdrawn at various intervals (60, 120, 180, 240 & 300 min) of time, centrifuged and used to evaluate the degradation of dye. The absorbance spectrum of the supernatant was subsequently measured using UV-Vis spectrophotometer. Concentration of dye during degradation was calculated by the absorbance value at 664nm. Percentage of dye degradation (decolourization) was estimated by the following formula:

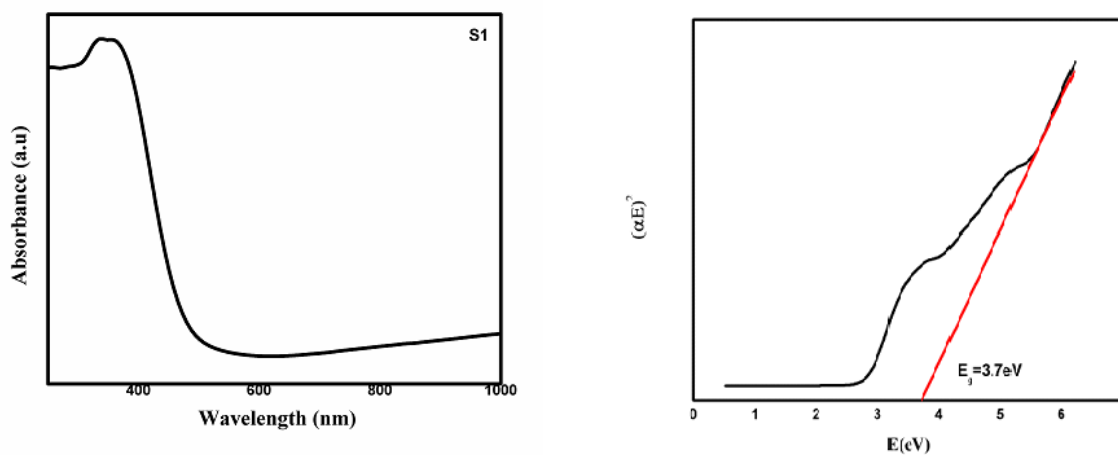
$$\% \text{ Decolourization} = \frac{100(C_0 - C)}{C_0}$$

Where C₀ is the initial concentration of dye solution and C is the concentration of dye solution during irradiation[4].

III. Results and Discussion

3.1 UV-Visible absorption Spectra

The optical absorption spectra of synthesized Ceria NPs were recorded in the wavelength range between 200nm and 800 nm. Figure 1(a) and (b) displays an optical absorption band peak of ceria nanoparticles obtained from muskmelon (sample 1-S1) and watermelon extract (sample 2-S2) at about 340nm and 344nm respectively. This peak is of typical absorption peak for metallic nanoceria cluster.



(a)

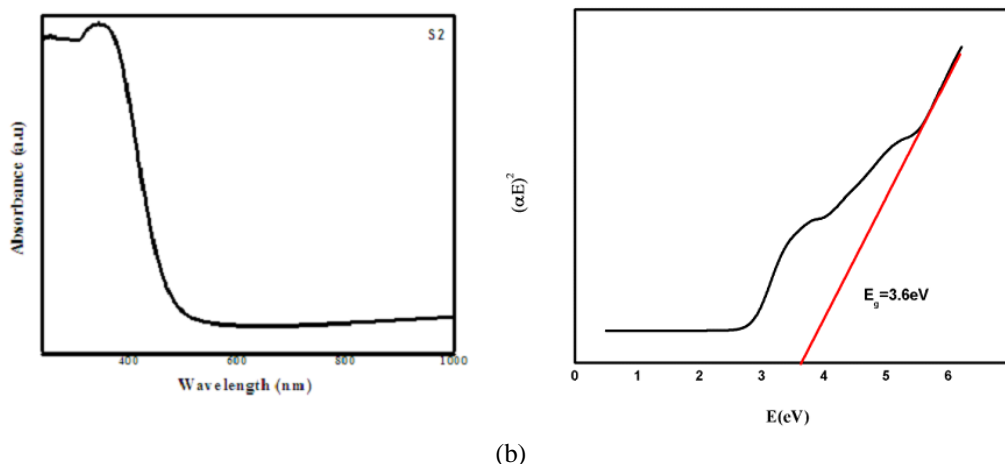


Fig.1. Absorption peak of Ceria NPs synthesized from (a) Muskmelon fruit extract (S1) and (b) Watermelon fruit extract (S2)

Ceria generally absorbs strongly in the UV-region. However, the energy bands may change accordingly with respect to confinement effect of the Nanomaterials[14]. The charge transfer between O-2p and Ce-4f states in ceria induce a strong absorbance between 270 – 350 nm[15]. The band gap of the synthesized nanoparticles can be determined by fitting the absorption data to the direct transition equation by extrapolating the linear portions of the curves to absorption equal to zero.

$$\alpha h\nu = A (h\nu - E_g)^{1/2}$$

where α is the optical absorption coefficient, $h\nu$ is the photon energy, E_g is the direct band gap, and A is a constant. The estimated band gap of the samples S1 and S2 are to be 3.7 eV and 3.6 eV respectively. It can be seen that the ceria samples show an increase in E_g compared to the bulk CeO₂ powders ($E_g = 3.19$ eV). The reason of increase in the optical band gap of synthesized Ceria NPs may due to their quantum confinement effect.

3.2 X-Ray Powder Diffraction

Figure 2 shows X-RD Pattern of the fruit extract derived Ceria nanoparticles (sample 1 and sample 2). It is observed that presence of four intense peaks in the whole spectrum of 2θ values ranging from 20° to 80° . The characteristic peaks corresponding to the (111), (200), (220), (311), (222), (400), and (331) planes are located at $2\theta \approx 29^\circ, 33^\circ, 47^\circ, 57^\circ, 59^\circ, 69^\circ$ and 76.7° , respectively.

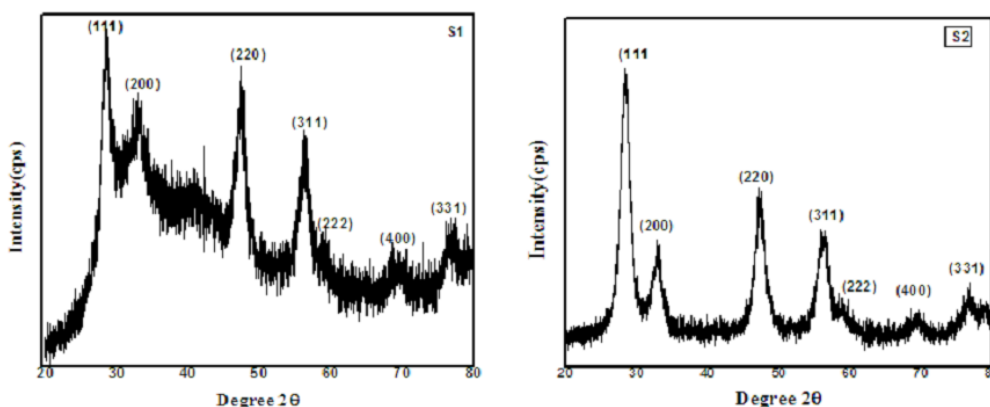


Fig.2. XRD Pattern of the Ceria NPs synthesized from Muskmelon fruit extract (S1) and Watermelon fruit extract (S2)

The Observed peak for Ceria NPs matches with the JCPDS values [(01-089-8436)]. Hence, the XRD patterns clearly show that the synthesized ceriumoxide nanoparticles S1 and S2 are identical and could be indexed to the standard ceria with face centered cubic structure. The lattice parameter calculated from the (111) reflection of the synthesized nanoparticles S1 (5.428 Å) and S2 (5.402 Å) agree with the lattice parameter of the bulk CeO₂ ($a = 5.412$ Å)[16,17]. Absence of any other characteristic peak in the spectrum indicates that the

synthesized nanoparticles are of pure in nature[11]. The average particle size of Ceria NPs can be calculated using the Debye- Scherrer's equation,

$$D = k\lambda / \beta \cos \theta$$

where's k is the Scherrer's constant with the value from 0.9 to 1 (shape factor), λ is the X- ray wavelength (1.5418 Å), β is the width of the X-RD peak at half- height and θ is the Bragg angle and D the grain size.

The average size of the synthesized Ceria nanoparticles of S1 and S2 calculated by the Scherrer equation is 27 nm and 20nm respectively.

3.3 FTIR analysis

FTIR spectroscopy is used to identify the functional groups and study the vibrational motion of atoms and molecules. Figure 3 shows the FTIR spectrum of sample 1 and sample 2 which are acquired in the range of 400–4000 cm^{-1} .

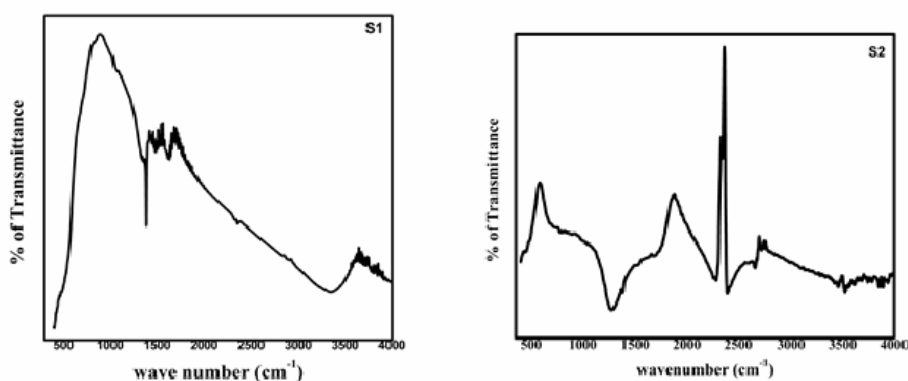


Fig.3.FTIR spectra of synthesized Ceria NPs synthesized from Muskmelon (S1) and Watermelon (S2) fruit extracts

Figure 3 shows the FTIR spectrum of the samples S1 and S2 which wereacquired in the range of 400–4000 cm^{-1} . FTIR spectrum of S1 and S2 showed peak at 449 cm^{-1} isdue to O-Ce-O stretching vibration[11]. The bands at 1068 and 1379 cm^{-1} are the characteristicspeaks due to stretching vibrations of C=O and C–O, respectively. The peak around 2355 cm^{-1} is the stretching vibration mode of O=C=O. The peaks at 1282, 1500, 1625 and 2659 cm^{-1} are dueto the C–N, N–O,C=O and C–H stretching vibration respectively. The broad band at 3456 cm^{-1} which is related to the O–H stretchingvibration of hydrated and physically absorbed H_2O in the sample[4]. The observed functional groups present in ceria nanoparticles are a result of the organic compounds like amino acids, vitamins and phenol compounds present in the fruit extract of muskmelon and watermelon.[3]

3.4 Raman studies

The structure of the Ceria nanoparticles was further elucidated byusing Raman spectroscopy which is shown in figure 4.

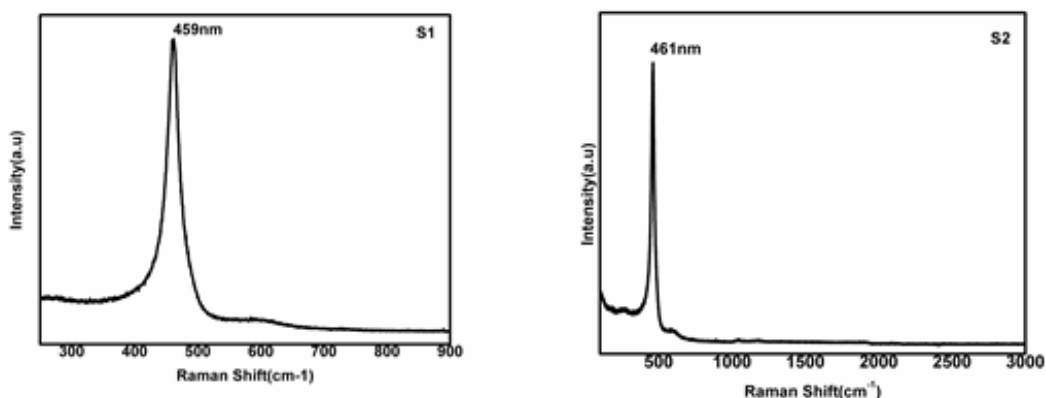


Fig.4. Raman spectrum of synthesized ceria nanoparticles from Muskmelon (S1) and Watermelon fruit extract (S2)

S1 and S2 exhibited a strong intense band at 459cm^{-1} and 461cm^{-1} which are generally correspond to the F_{2g} Raman active-mode of fluorite type cubic structure [11,17]. It is attributed to a symmetrical stretching mode of the Ce-O vibrational unit [18]. Raman spectrum thus confirm that the synthesized products have well crystalline fluorite cubic structure.

3.5 Degradation study of Methylene Blue dye

Exposure of aqueous solution of Methylene blue dye in the presence of ceria nanoparticles of S1 and S2 under sunlight lead to change in the absorbance as a function of irradiation time. Figure 5 represents the change in the absorbance spectra for the photocatalytic degradation of MB in the presence of S1 and S2 at different time intervals respectively.

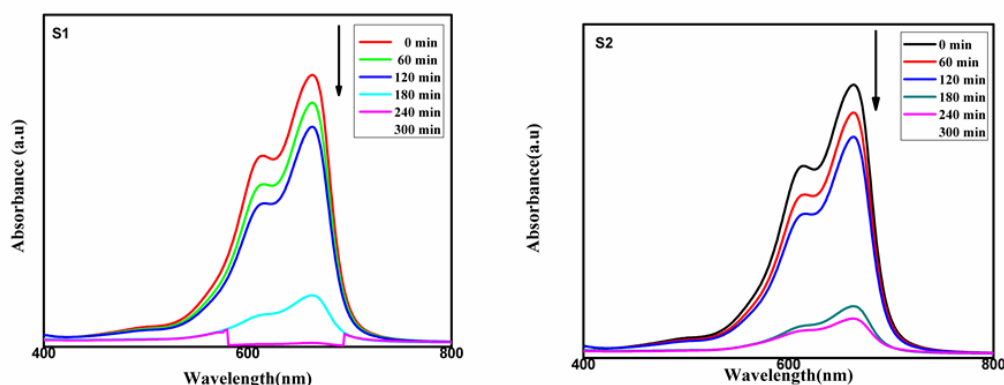


Fig.5. Change in absorption spectrum of MB in the presence of (a) S1 and (b) S2 at different irradiation time.

It is observed that irradiation of aqueous suspension of MB dye in the presence of ceria nanoparticles leads to decrease in absorption intensity. It can be seen that the maximum absorbance at 664 nm gradually decreases with increase in irradiation time. Figure 6 shows the plot for the % degradation versus irradiation time (min) of MB solution in the presence of S1 and S2. It could be seen that 91% of MB is degraded in the presence of S1 whereas 100% degradation occurs in case of S2 after 300 min of irradiation time.

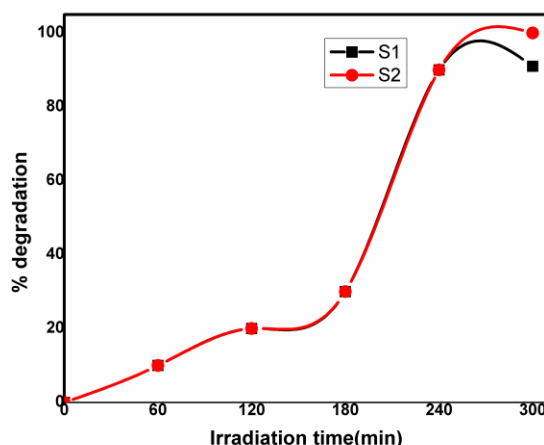


Fig.6. Percentage of degradation of dye in the presence of S1 and S2

The dependence of adsorption on contact time was studied using fixed amount (0.01 g) of adsorbent (CeriaNPs) and (0.01 g) of methylene blue on 100 ml distilled water solution in a fixed volume. It was observed that adsorption increases with increase in contact time. For each sample, the degradation rate constant for the decomposition of MB was calculated. The kinetics of MB decolorization on S1 and S2 are presented in figure 7, and are found to follow pseudo-first order reaction as shown in equation

$$-\ln(C/C_0) = Kt$$

where k is the apparent rate constant (min^{-1}), C_0 is the initial concentration of dye and C is the concentration of dye at time t [11,19].

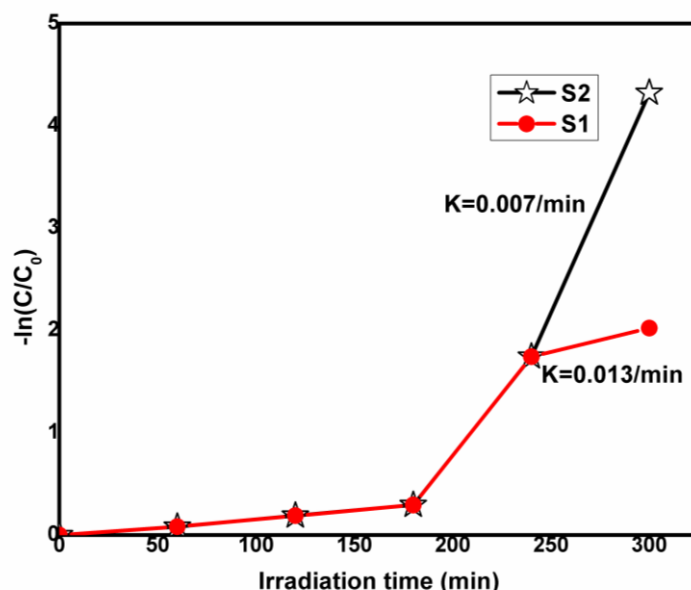


Fig.7.The kinetics plot for pseudo first order reaction of MB decolorization

As the dye concentration remains same, it can be substituted by the dye absorbance at a given wavelength (typically the peak absorption). And it is observed that the rate constant of S2 is slightly lower than that of S1.

In the present study, heterogeneous photocatalysis mechanism is involved for the degradation of Methylene Blue (MB) dye. The formation of electron and hole pair will take place on exposure of light to Ceria NPs if the incident light has energy equal to or greater than the band gap of Ceria NPs. The electron and hole migrate to the surface of metal oxide [11]. The migrated hole reacts with MB dye results in its oxidation producing CO_2 and H_2O as end products. It also produces hydroxyl radical ($\cdot\text{OH}$) while reacting with water. The electron in the conductive band reacts with oxygen forming a superoxide radical ($\text{O}_2^{\cdot-}$). Hydroxyl radicals ($\cdot\text{OH}$) and superoxide radical anions ($\text{O}_2^{\cdot-}$) are supposed to be the main destructive agents (oxidizing species) and these oxidative reaction results in the oxidation of the dyes, often up to complete mineralization [20,21].

The whole mechanism of photoactivity of synthesized Ceria nanoparticles is depicted in Figure 8. Hence, Ceria nanoparticles can be used as an efficient photocatalyst in large scale under the sunlight illumination for the degradation of water pollutant and the environmental pollution [16].

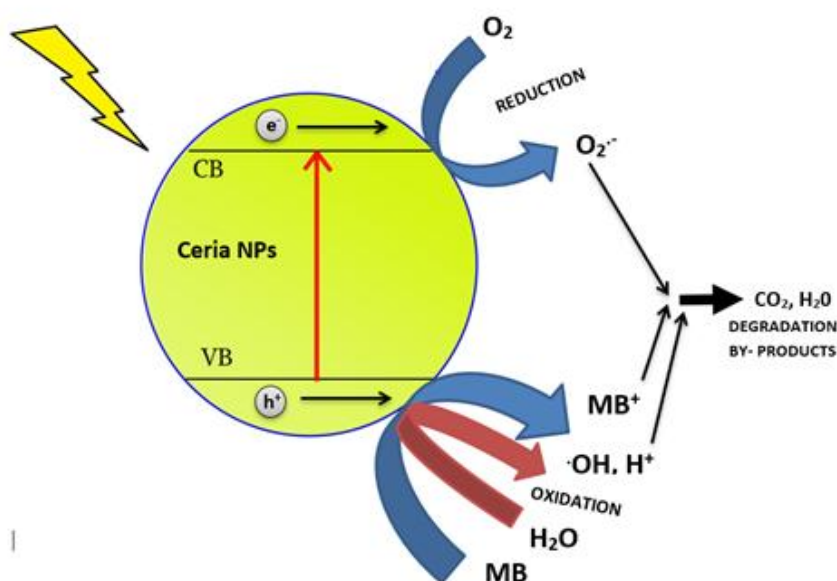


Fig.8. Mechanism of the degradation of MB dye using Ceria nanoparticles.

IV. Conclusion

Ceria Nanoparticles had been synthesized using fruit extract of Muskmelon(S1)and Watermelon(S2). The synthesized Ceria Nanoparticles were characterized using UV-Visible spectrophotometer, XRD, FT-IR and Raman spectrometer. Crystalline nature was characterized by XRD. FTIR spectrum was used to identify the effective functional molecules responsible for the reduction and stabilization of Ceria nanoparticles synthesized by fruit extract. It was observed that Ceria nanoparticles showed significant photocatalytic activity leading to the degradation of Methylene blue dye under sun light. The main absorption peak of methylene blue dye at 664nm decreased gradually with the extension of the exposure time. 91% of MB is degraded in the presence of S1 whereas 100% degradation occurs in case of S2 after 300 min of irradiation time. It is concluded that the Ceria nanoparticles synthesized from fruit extract can be one of the best candidates for environmental applications as a photo-catalyst.

This research did not receive any specific grant from funding agencies in the public, commercial, or not-for-profit sectors.

References:

- [1]. F. Charbgo, M. Bin Ahmad, M. Darroudi, Cerium oxide nanoparticles: Green synthesis and biological applications, *International Journal of Nanomedicine*. (2017). <https://doi.org/10.2147/IJN.S124855>.
- [2]. G. Sai Priya, A. Kanneganti, K. Anil Kumar, K. Venkateswara Rao, S. Bykkam, Bio Synthesis of Cerium Oxide Nanoparticles using Aloe Barbadensis Miller Gel, *International Journal of Scientific and Research Publications*. 4 (2014) 1–4. www.ijsrp.org.
- [3]. T. Masui, H. Hirai, N. Imanaka, G. Adachi, T. Sakata, H. Mori, Synthesis of cerium oxide nanoparticles by hydrothermal crystallization with citric acid, *Journal of Materials Science Letters*. 21 (2002) 489–491. <https://doi.org/10.1023/A:1015342925372>.
- [4]. L.S. Reddy Yadav, K. Manjunath, B. Archana, C. Madhu, H. Raja Naika, H. Nagabhushana, C. Kavitha, G. Nagaraju, Fruit juice extract mediated synthesis of CeO₂ nanoparticles for antibacterial and photocatalytic activities, *European Physical Journal Plus*. 131 (2016). <https://doi.org/10.1140/epjp/i2016-16154-y>.
- [5]. M. Nyoka, Y.E. Choonara, P. Kumar, P.P.D. Kondiah, V. Pillay, Synthesis of cerium oxide nanoparticles using various methods: Implications for biomedical applications, *Nanomaterials*. 10 (2020). <https://doi.org/10.3390/nano10020242>.
- [6]. Q. Yuan, H.H. Duan, L. Le Li, L.D. Sun, Y.W. Zhang, C.H. Yan, Controlled synthesis and assembly of ceria-based nanomaterials, *Journal of Colloid and Interface Science*. 335 (2009) 151–167. <https://doi.org/10.1016/j.jcis.2009.04.007>.
- [7]. N.M. Zholobak, V.K. Ivanov, A.B. Shcherbakov, A.S. Shaporev, O.S. Polezhaeva, A.Y. Baranchikov, N.Y. Spivak, Y.D. Tretyakov, UV-shielding property, photocatalytic activity and photocytotoxicity of ceria colloid solutions, *Journal of Photochemistry and Photobiology B: Biology*. 102 (2011) 32–38. <https://doi.org/10.1016/j.jphotobiol.2010.09.002>.
- [8]. S.A. Mahmud, Biosynthesis of CeO₂ NPs using the optimal extract of *Moringa olifera*, 10 (2016) 37–39.
- [9]. S. Munusamy, K. Bhagyaraj, L. Vijayalakshmi, A. Stephen, V. Narayanan, Synthesis and characterization of cerium oxide nanoparticles using *Curvularia lunata* and their antibacterial properties, *Int J Innovative Res Sci Eng*. 12 (2014) 1401–1413. <https://pdfs.semanticscholar.org/b3b8/22ad2cb5818960345dcb2ee5a0666fac1aae.pdf>.
- [10]. H.R. Pourtedal, A. Kadkhodaie, Synthetic CeO₂ nanoparticle catalysis of methylene blue photodegradation: Kinetics and mechanism, *Cuihua Xuebao/Chinese Journal of Catalysis*. 31 (2010) 1328–1334. [https://doi.org/10.1016/s1872-2067\(10\)60121-0](https://doi.org/10.1016/s1872-2067(10)60121-0).
- [11]. S.K. Kannan, M. Sundarajan, A green approach for the synthesis of a cerium oxide nanoparticle: Characterization and antibacterial activity, *International Journal of Nanoscience*. 13 (2014) 1–7. <https://doi.org/10.1142/S0219581X14500185>.
- [12]. Muhammad Umar and Hamidi Abdul Aziz, *Organic Pollutants - Monitoring, Risk and Treatment*, 2013th ed., InTech, 2013. <https://doi.org/10.5772/55953>.
- [13]. Á. Guzmán Aponte, M. A Llano Ramírez, Y. Cadavid Mora, J. F Santa Marín, R. Buitrago Sierra, Cerium oxide nanoparticles for color removal of indigo carmine and methylene blue solutions, *AIMS Materials Science*. 7 (2020) 468–485. <https://doi.org/10.3934/matricsci.2020.4.468>.
- [14]. B. Choudhury, A. Choudhury, Ce³⁺ and oxygen vacancy mediated tuning of structural and optical properties of CeO₂ nanoparticles, *Materials Chemistry and Physics*. 131 (2012) 666–671. <https://doi.org/10.1016/j.matchemphys.2011.10.032>.
- [15]. K.K. Babitha, A. Sreedevi, K.P. Priyanka, B. Sabu, T. Varghese, Structural characterization and optical studies of CeO₂ nanoparticles synthesized by chemical precipitation, *Indian Journal of Pure and Applied Physics*. 53 (2015) 596–603.
- [16]. S.B. Khan, M. Faisal, M.M. Rahman, A. Jamal, Exploration of CeO₂ nanoparticles as a chemi-sensor and photo-catalyst for environmental applications, *Science of the Total Environment*. 409 (2011) 2987–2992. <https://doi.org/10.1016/j.scitotenv.2011.04.019>.
- [17]. N. Thovhogi, A. Diallo, A. Gurib-Fakim, M. Maaza, Nanoparticles green synthesis by *Hibiscus Sabdariffa* flower extract: Main physical properties, *Journal of Alloys and Compounds*. 647 (2015) 392–396. <https://doi.org/10.1016/j.jallcom.2015.06.076>.
- [18]. A. Arumugam, C. Karthikeyan, A.S. Haja Hameed, K. Gopinath, S. Gowri, V. Karthika, Synthesis of cerium oxide nanoparticles using *Gloriosa superba* L. leaf extract and their structural, optical and antibacterial properties, *Materials Science and Engineering C*. 49 (2015) 408–415. <https://doi.org/10.1016/j.msec.2015.01.042>.
- [19]. L.S.R. Yadav, R. Thippeswamy, P. Shekarappa, R.G. Kempegowda, N. Ganganagappa, Photocatalytic Activities, Kinetics and Adsorption Isotherm Studies of CeO₂ Nanoparticles Synthesized via Low Temperature Combustion Method, *Current Nanomaterials*. 4 (2019) 223–234. <https://doi.org/10.2174/2405461504666191011171031>.
- [20]. T.N. Ravishankar, T. Ramakrishnappa, G. Nagaraju, H. Rajanaika, Synthesis and Characterization of CeO₂ Nanoparticles via Solution Combustion Method for Photocatalytic and Antibacterial Activity Studies, *ChemistryOpen*. (2015). <https://doi.org/10.1002/open.201402046>.
- [21]. B. Elahi, M. Mirzaee, M. Darroudi, R. Kazemi Oskuee, K. Sadri, L. Gholami, Role of oxygen vacancies on photo-catalytic activities of green synthesized ceria nanoparticles in *Cydonia oblonga miller* seeds extract and evaluation of its cytotoxicity effects, *Journal of Alloys and Compounds*. 816 (2020) 152553. <https://doi.org/10.1016/j.jallcom.2019.152553>.

SuvethaRani.J. "Synthesis of Ceria nanoparticles for the photocatalytic degradation of Methylene Blue dye using fruit extracts." *IOSR Journal of Applied Physics (IOSR-JAP)*, 12(6), 2020, pp. 35-41.